Joint Bone Spine 86 (2019) 665–668

Available online at
ScienceDirect
www.sciencedirect.com

Elsevier Masson France
EM|consulte
www.em-consulte.com/en

Editorial

Winds of change in imaging of calcium crystal deposition diseases

ARTICLE INFO

Keywords:
Calcium hydroxyapatite
Calcium pyrophosphate
Crystals
Dual-energy CT
Multi-energy spectral photon-counting CT

Calcium pyrophosphate (CPP) and basic calcium phosphate (BCP, which include carbonate-substituted calcium hydroxyapatite (HA) and octacalcium phosphate) are the two most common types of calcium-containing crystals involved in musculoskeletal diseases [1,2]. CPP-related arthritis is the third most common inflammatory arthritis while calcium pyrophosphate deposition (CPPD) prevalence, which is underestimated at ~0.4% of the overall population when defined by radiographic chondrocalcinosis [3], is increasing with the aging population [4]. Tissue deposition of calcium crystals is associated with a wide variety of articular and periarticular disorders, ranging from acute CPP crystal arthritis (also referred to as "pseudogout") to chronic CPP crystal inflammatory arthritis with or without osteoarthritis for CPP, and from acute calcific tendonitis and periarthritis to large-joint destructive arthropathies such as Milwaukee shoulder syndrome and possibly osteoarthritis for BCP [1,2,4]. While calcium oxalate is the most common type of urinary stones [5] and can also be found in breast microcalcifications (type I) of benign ductal cysts [6], it remains a rare cause of crystal arthritis [7].

Until recently, imaging of calcium crystal deposition diseases was limited to traditional methods such as plain radiography, ultrasound (US), and conventional ("single-energy") computed tomography (CT). Making use of the classic morphological radiographic features (linear opacities for CPP versus amorphous and cloud-like for HA) to detect and characterize the various calcium crystals certainly helps [8], but yields only moderate diagnostic accuracy (sensitivity as low as 29% for radiographic chondrocalcinosis in certain circumstances) [4], as does the application of the anatomical compartment-based approach [9]. Although in recent years US has sparked growing interest for the diagnosis of CPPD in peripheral joints, owing in particular to its high sensitivity (outperforming plain radiography in certain cases) [2,4,10], this widely available technique provides only limited potential for discriminating between the different types of calcium crystals. Furthermore, the US features of CPPD vary widely and the outcome measures in rheumatology (OMERACT) US definitions for CPP deposits in joints and periarticular tissues are based on expert opinion [11]. No study has yet conclusively proven that US detected abnormalities are indeed pure CPP and not a mixture of CPP and BCP crystal aggregates. Therefore, these definitions would now benefit from further validation using highly specific crystal analytic methods such as Raman and Fourier-transform infrared spectroscopy. On the other hand, even though conventional CT has the potential to map and quantify calcium crystal deposition in vivo and is more accurate and reliable than plain radiography overall, as well as US when assessing deep joint structures or axial skeletal involvement specifically [2,12,13], this technique is not able to readily differentiate CPP from BCP crystal aggregates. Hence, the definitive diagnosis of CPPD remains to date by microscopic identification of characteristic CPP crystals in synovial fluid [4], while BCP crystals are undetectable individually by conventional or compensated polarized light microscopy and necessitate advanced crystal identification methods [1].

Accurate detection and characterization of calcium crystal types by imaging pose major challenges. First, the small size of crystals (1–20 μm for CPP versus 20–100 nm for BCP individually [1,2]) means that only aggregates may be detected with clinically available imaging systems (highest spatial resolution/detector elements of ~100 μm for 2D systems), thereby preventing early diagnosis of calcium crystal deposition diseases. Secondly, CPP and BCP crystals hold similar molecular formulas with comparable physical and chemical properties, thus requiring advanced methods to discriminate them. Despite existing spectroscopic differences (as identified using Raman or Fourier-transform infrared spectroscopy) between the various calcium compounds, the k-edge of calcium (4.0 keV) is too low to be exploited with current clinical imaging techniques operating in the human energy range (Fig. 1) [14]. Among emerging imaging techniques, first dual-energy CT (DECT) [15,16] and more recently multi-energy spectral photon-counting CT (SPCCT) [14,17] have both shown promise.

In brief, DECT is based on the principle that x-ray tissue attenuation (represented by CT numbers within each voxel, in Hounsfield units (HU)) depends on material composition (represented by its effective atomic number (Z_{eff})), its density (in g/cm^3), and the effective energy of the polychromatic x-ray photon beam (in keV) [18]. In the clinical CT energy range, tissue attenuation is primarily due to Compton scattering and photoelectric absorption. While Compton scattering mainly depends on electron density, which is correlated with volumetric mass density, it does not depend on x-ray energy. Conversely, photoelectric absorption heavily depends on both material composition (Z_{eff}) and x-ray energy. Therefore,

https://doi.org/10.1016/j.jbspin.2019.04.005

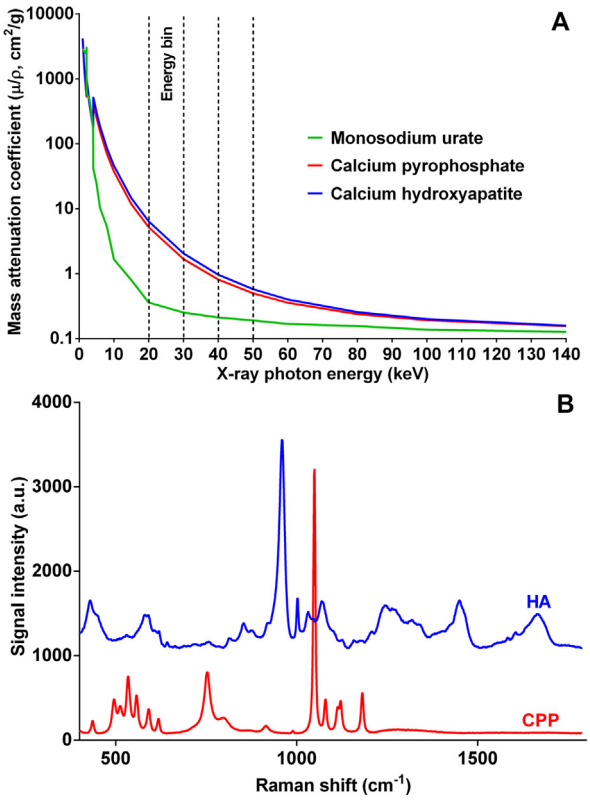

Fig. 1. (A, top) Mass attenuation coefficients as a function of the x-ray photon energy for monosodium urate, calcium pyrophosphate and calcium hydroxyapatite, generated from the National Institute of Standards and Technology database. Adapted from [14]. (B, bottom) Raman spectra for calcium pyrophosphate (CPP) and calcium hydroxyapatite (HA) crystals from patient samples.

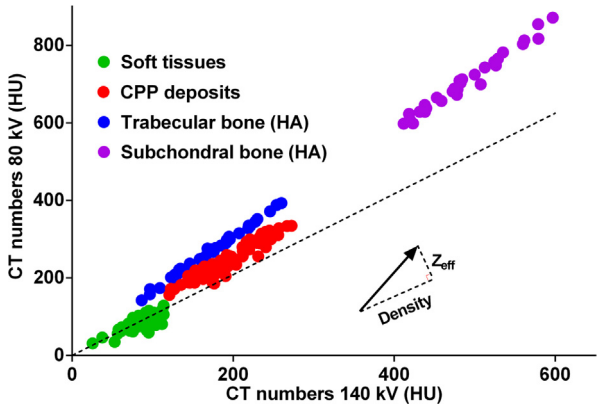

Fig. 2. CT numbers as a function of the tube potential for soft tissues, calcium pyrophosphate (CPP) deposits, and calcium hydroxyapatite (HA) in trabecular and subchondral bone. Z_{eff}: effective atomic number. Adapted from [18].

photoelectric absorption is the predominant factor to consider for material differentiation using DECT. Fig. 2 illustrates the specific effects of Z_{eff} (photoelectric absorption) and density (Compton scattering) on CT numbers at high and low energies (typically 140 and 80 kV, respectively). The slope of a material/tissue corresponds to its Z_{eff}, while the distance from the origin represents its density. The potential for material differentiation with DECT mainly depends on the slope difference between two materials of interest: the greater the difference, the better the discrimination.

Over the past decade, DECT has been increasingly used in crystal arthritis imaging, almost exclusively in gout [19]. Few studies have indeed explored the potential of DECT in calcium crystal deposition diseases. Diekhoff et al. initially aimed to determine the lowest concentrations of monosodium urate (MSU) and CPP detectable and characterizable in vitro using DECT [15]. They reported reliable limits of detection for MSU and CPP at relatively low concentrations (≥ 12.5% and ≥ 6.25%, respectively), corresponding to soft tissue crystal deposits with mean CT numbers of 59.8 and 101.1 HU, respectively. In a subsequent ex vivo investigation, Tanikawa et al. compared the diagnostic accuracy of DECT and plain radiography for identifying CPP crystal deposits in knee menisci harvested during total knee arthroplasty, using polarized light microscopy of synovial fluid aspirates as reference standard [16]. They found that DECT was more sensitive (77.8% versus 44.4%, respectively) but less specific (93.8% versus 100%, respectively) than plain radiography. More recently, an initial clinical study determined the DECT attenuation characteristics of meniscal calcifications in CPPD patients, and assessed whether DECT was able to discriminate meniscal CPP deposits from calcium HA in subchondral and trabecular bone in vivo [20]. The authors found that meniscal CPP deposits were readily distinguished from subchondral and trabecular bone HA, mainly owing to Z_{eff} differences between these two calcium compounds.

Multi-energy SPCCT is a novel advanced imaging technique currently being translated to human imaging and having the potential to revolutionize clinical CT use in the coming decades. By using energy-resolving instead of energy-integrating detectors as in conventional CT and DECT, SPCCT systems are able to count individual incoming photons from a single x-ray beam and measure their energy in separate bins [21]. System performance in SPCCT highly depends on the scanner manufacturer. When broadly compared with current CT technology, SPCCT will allow for reduced image noise (by eliminating electronic noise) with increased signal- and contrast-to-noise ratios, improved spatial resolution (~100 μm), and spectral imaging of heavy atom contrast agents. All this should eventually result in radiation dose reductions of ~20–40%, depending on the diagnostic imaging tasks, while opening up new horizons for quantitative spectral/molecular CT imaging.

Initial in vitro followed by ex vivo investigations have shown promising results in identifying various calcium crystals. By using a commercially available SPCCT system (MARS Bioimaging Ltd, Christchurch, New Zealand) that has ~110 μm detector elements, up to 8 energy bins, and an energy resolution of ~2.5 keV (full width at half maximum) by mitigating the charge sharing effect through inter-pixel communication, Kirkbride et al. first aimed to determine in vitro whether SPCCT could distinguish between several concentrations of calcium HA and calcium oxalate at clinical x-ray energy ranges [14]. They reported that the two lower concentrations of HA (54.3 and 211.7 mg/cm^3) were distinguishable from oxalate (2000 mg/cm^3) with all tested SPCCT protocols, while discrimination at higher concentrations (808.5 and 1169.3 mg/cm^3) depended primarily on the energy thresholds used. A subsequent in vitro study evaluated the diagnostic performance of this SPCCT imaging technique (MARS Bioimaging Ltd) in a crystal arthritis experimental setup [22]. Overall, the authors found that the differentiation of MSU from CPP and HA was excellent (sensitivity, 95.7–97.8%; specificity, 97.0–99.0%), while the distinction between CPP and HA was only moderate and more challenging (sensitivity, 56.4%; specificity, 88.5%) (Fig. 3). Most recently, Stamp et al. assessed whether SPCCT (MARS Bioimaging Ltd) could detect and differentiate between MSU, CPP and calcium HA crystal deposits ex vivo [17]. Although DECT and SPCCT both identified MSU deposits in an excised finger with a subcutaneous tophus, SPCCT was able to detect finer detail. On the other hand, plain radiography of an excised osteoarthritic calcified meniscus identified chondrocalcinosis consistent with CPP, while SPCCT detected and differentiated both CPP and calcium HA deposits.

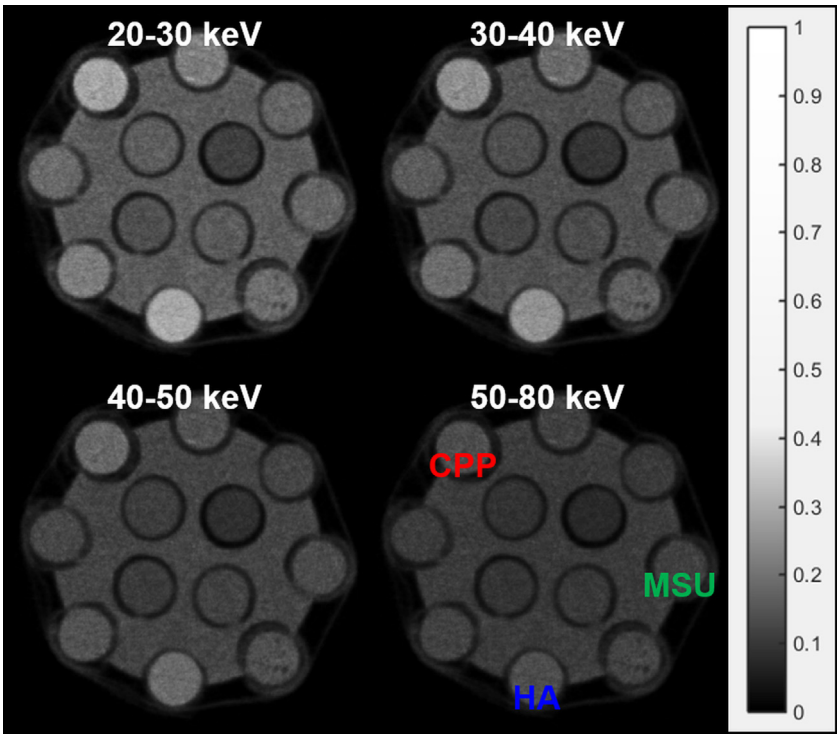

Fig. 3. Multi-energy SPCCT images as a function of the energy bin for synthetic crystals of monosodium urate (MSU), calcium pyrophosphate (CPP) and calcium hydroxyapatite (HA). Adapted from [17].

In conclusion, owing to the latest technological advances in imaging, we are in the process of moving from grayscale conventional radiography and CT to material-specific quantification and mapping of color-coded crystal deposits with DECT and multi-energy SPCCT. There is potential for SPCCT to become useful in the diagnosis of crystal arthritis and calcific periarthritis/tendonitis, and to provide a better understanding and deeper insights into the possibly pathogenic role that various calcium crystals play within joints in vivo, including in osteoarthritis.

Disclosure of interest

L.S. has received speaker fees from Amgen unrelated to the current work. A.R. has accepted the share option of MARS Bioimaging Ltd., a company that manufactures the MARS SPCCT scanner.

The other authors declare that they have no competing interest.

Acknowledgments

The authors gratefully acknowledge Maya Rajeswari, Bradon Noordanus and Guillaume Falgayrac for their help in preparing the figures. The MARS Collaboration received funding from the Ministry of Business, Innovation and Employment (MBIE), New Zealand under contract number UOCX1404, and the Ministry of Education through the MedTech CoRE.

References

[1] McCarthy GM, Dunne A. Calcium crystal deposition diseases – beyond gout. Nat Rev Rheumatol 2018;14:592–602, http://dx.doi.org/10.1038/s41584-018-0078-5.
[2] Ea HK, Lioté F. Diagnosis and clinical manifestations of calcium pyrophosphate and basic calcium phosphate crystal deposition diseases. Rheum Dis Clin North Am 2014;40:207–29, http://dx.doi.org/10.1016/j.rdc.2014.01.011.
[3] Salaffi F, De Angelis R, Grassi W. MArche Pain Prevalence, Investigation Group (MAPPING) study. Prevalence of musculoskeletal conditions in an Italian population sample: results of a regional community-based study. I. The MAPPING study. Clin Exp Rheumatol 2005;23:819–28.
[4] Zhang W, Doherty M, Bardin T, et al. European League Against Rheumatism recommendations for calcium pyrophosphate deposition. Part I: terminology and diagnosis. Ann Rheum Dis 2011;70:563–70, http://dx.doi.org/10.1136/ard.2010.139105.
[5] Lieske JC, Rule AD, Krambeck AE, et al. Stone composition as a function of age and sex. Clin J Am Soc Nephrol 2014;9:2141–6.
[6] Radi MJ. Calcium oxalate crystals in breast biopsies. An overlooked form of microcalcification associated with benign breast disease. Arch Pathol Lab Med 1989;113:1367–9.
[7] Lorenz EC, Michet CJ, Milliner DS, et al. Update on oxalate crystal disease. Curr Rheumatol Rep 2013;15:340.
[8] Freire V, Moser TP, Lepage-Saucier M. Radiological identification and analysis of soft tissue musculoskeletal calcifications. Insights Imaging 2018;9:477–92.
[9] Banks KP, Bui-Mansfield LT, Chew FS, et al. A compartmental approach to the radiographic evaluation of soft-tissue calcifications. Semin Roentgenol 2005;40:391–407.
[10] Filippou G, Adinolfi A, Iagnocco A, et al. Ultrasound in the diagnosis of calcium pyrophosphate dihydrate deposition disease. A systematic literature review and a meta-analysis. Osteoarthritis Cartilage 2016;24:973–81.
[11] Filippou G, Scirè CA, Damjanov N, et al. Definition and reliability assessment of elementary ultrasonographic findings in calcium pyrophosphate deposition disease: a study by the OMERACT calcium pyrophosphate deposition disease ultrasound subtask force. J Rheumatol 2017;44:1744–9.
[12] Touraine S, Ea HK, Bousson V, et al. Chondrocalcinosis of femoro-tibial and proximal tibio-fibular joints in cadaveric specimens: a high-resolution CT imaging study of the calcification distribution. PLoS One 2013;8:e54955.
[13] Misra D, Guermazi A, Sieren JP, et al. CT imaging for evaluation of calcium crystal deposition in the knee: initial experience from the Multicenter Osteoarthritis (MOST) study. Osteoarthritis Cartilage 2015;23:244–8.
[14] Kirkbride TE, Raja AY, Müller K, et al. Discrimination between calcium hydroxyapatite and calcium oxalate using multienergy spectral photon-counting CT. AJR Am J Roentgenol 2017;209:1088–92.
[15] Diekhoff T, Kiefer T, Stroux A, et al. Detection and characterization of crystal suspensions using single-source dual-energy computed tomography: a phantom model of crystal arthropathies. Invest Radiol 2015;50:255–60.
[16] Tanikawa H, Ogawa R, Okuma K, et al. Detection of calcium pyrophosphate dihydrate crystals in knee meniscus by dual-energy computed tomography. J Orthop Surg 2018;13:73.
[17] Stamp LK, Anderson NG, Becce F, et al. Clinical utility of multi-energy spectral photon-counting CT in crystal arthritis. Arthritis Rheumatol 2019, http://dx.doi.org/10.1002/art.40848.
[18] Omoumi P, Becce F, Racine D, et al. Dual-energy CT: Basic principles, technical approaches, and applications in musculoskeletal imaging (Part 1). Semin Musculoskelet Radiol 2015;19:431–7.
[19] Omoumi P, Verdun FR, Guggenberger R, et al. Dual-energy CT: basic principles, technical approaches, and applications in musculoskeletal imaging (Part 2). Semin Musculoskelet Radiol 2015;19:438–45.

[20] Pascart T, Norberciak L, Legrand J, et al. Dual-energy computed tomography in calcium pyrophosphate deposition: initial clinical experience. Osteoarthritis Cartilage 2019, http://dx.doi.org/10.1016/j.joca.2019.05.007.
[21] Willemink MJ, Persson M, Pourmorteza A, et al. Photon-counting CT: technical principles and clinical prospects. Radiology 2018;289:293–312.
[22] Viry A, Raja AY, Kirkbride TE, et al. Multi-energy spectral photon-counting CT in crystal-related arthropathies: initial experience and diagnostic performance in vitro. Proceedings volume 10573, Medical Imaging 2018. Phys Med Imaging 2018;1057351, http://dx.doi.org/10.1117/12.2293458.

Fabio Becce[a,*]
Anais Viry[b]
Lisa K. Stamp[c]
Tristan Pascart[d,e]
Jean-François Budzik[e,f]
Aamir Raja[g,h], MARS Collaboration[1]
[a] *Department of diagnostic and interventional radiology, Lausanne University Hospital and University of Lausanne, 1011 Lausanne, Switzerland*
[b] *Institute of radiation physics, Lausanne University Hospital and University of Lausanne, 1007 Lausanne, Switzerland*
[c] *Department of medicine, University of Otago, Christchurch 8140, New Zealand*
[d] *Department of rheumatology, Lille Catholic Hospitals, University of Lille, 59160 Lomme, France*
[e] *EA4490, physiopathologie des maladies osseuses inflammatoires, University of Lille, 59000 Lille, France*
[f] *Department of radiology, Lille Catholic Hospitals, University of Lille, 59160 Lomme, France*
[g] *Department of radiology, University of Otago, Christchurch 8011, New Zealand*
[h] *MARS Bioimaging Ltd, Christchurch, New Zealand*

[*] Corresponding author.
E-mail address: fabio.becce@chuv.ch (F. Becce)

[1] MARS collaboration : Sikiru A Adebileje, Steven D Alexander, Maya R Amma, Marzieh Anjomrouz, Fatemeh Asghariomabad, Ali Atharifard, James Atlas, Benjamin Bamford, Stephen T Bell, Srinidhi Bheesette, Anthony P H Butler, Philip H Butler, Pierre Carbonez, Claire Chambers, Alexander I Chernoglazov, Shishir Dahal, Jérôme Damet, Niels J A de Ruiter, Robert M N Doesburg, Neryda Duncan, Steven P Gieseg, Brian P Goulter, Sam Gurney, Joseph L Healy, Praveenkumar Kanithi, Tracy Kirkbride, Stuart P Lansley, Chiara Lowe, V B H Mandalika, Emmanuel Marfo, Aysouda Matanaghi, Mahdieh Moghiseh, David Palmer, Raj K Panta, Hannah M Prebble, Aamir Y Raja, Peter Renaud, Nanette Schleich, Emily Searle, Jereena S Sheeja, Rayhan Uddin, Lieza Vanden Broeke, Vivek V S, E Peter Walker, Michael F Walsh, Manoj Wijesooriya.

Available online 5 May 2019